groups, the NOE data indicate certain conformational preferences for the Lys and Gln side chains in the complex as depicted in Figure 5. The additional hydrophobic interactions associated with the Gln side chain and the aridicin core suggested by this NMR data, in conjunction with entropic effects associated with desolvation of the L-Ala[1] and L-α-Gln, may be important in accounting for the increased lifetime of the pentapeptide complex compared to the tripeptide complex.

Utilization of accurate volume integrals from the NOESY spectra obtained at two mixing times to derive $^1H-^1H$ distance information obviously has limitations in that the effects of spin diffusion are neglected. However the use of asymmetric distance bounds to compensate for the effects of spin diffusion proved successful in that six of the seven structures obtained by the use of a distance geometry algorithm showed a high degree of convergence, reflecting the correlation of the NMR distance constraints. On the basis of these results, we feel confident that, for structures that are comparable in their rigidity to aridicin aglycon, this method is capable of providing well-built model structures. Although it is less rigorous than procedures to monitor build-up rates that were used for a similar compound by Fesik and workers,[6] it has advantages in that while it is much simpler, it is capable of providing structural models of similar quality. An assessment of the validity of this latter statement may be obtained from a comparison of the distance information from this study and that reported by Fesik et al.[6] for the core region of ristocetin. Of the 17 NOE constraints that are tabulated for the core region of the complex of ristocetin aglycon and the tripeptide (**2**), only two fall outside the distance bounds derived for the aridicin aglycon complexes in the current study.[26] These deviations involve the interpeptide NOE's linking D-Ala[4] to G1′ and to E2. The values derived for the ristocetin complex are 0.3 and 0.5 Å longer than the upper bounds assigned for the aridicin A complex in this study.

The NMR data support the proposal of a single solution conformation of the aglycon irrespective of whether it is bound to the tripeptide (**2**) or the pentapeptide (**3**) and suggest that both **2** and **3** are good models for probing the binding interactions at the molecular level of this class of antibiotics to bacterial cell-wall intermediates.

The results of the current study, when used in conjunction with the analysis of the NMR constraints described in ref 24, make it possible to designate those regions of the structure that are well-defined by the distance information and also to make some predictions about regions that may be exhibiting more mobility or conformational diversity. We believe that the NMR methods described will be generally useful for obtaining well-built models of structures that do not contain structural regions exhibiting grossly different time scales of internal motion.

Studies of Rare-Earth Stannates by ^{119}Sn MAS NMR. The Use of Paramagnetic Shift Probes in the Solid State

Clare P. Grey,[†] Christopher M. Dobson,*[,‡] Anthony K. Cheetham,[†] and Roger J. B. Jakeman[†]

Contribution from the Chemical Crystallography Laboratory, University of Oxford, 9 Parks Road, Oxford OX1 3PD, U.K., and the Inorganic Chemistry Laboratory, University of Oxford, South Parks Road, Oxford OX1 3QR, U.K. *Received June 20, 1988*

Abstract: ^{119}Sn MAS NMR spectra have been obtained from members of a series of rare-earth stannates $Ln_2Sn_2O_7$ (Ln = La, Pr, Nd, Sm, Eu, Tm, Yb, Lu, and Y), all of which adopt the pyrochlore structure. Apart from $La_2Sn_2O_7$, $Lu_2Sn_2O_7$, and $Y_2Sn_2O_7$, these compounds are paramagnetic and exhibit a very large variation in ^{119}Sn chemical shifts (from approximately +5400 to −4200 ppm), which can be attributed principally to a Fermi contact shift mechanism. The spectra from the paramagnetic samples have large overall line widths associated with the substantial anisotropy of the shift, but the individual peaks within the spinning sideband manifolds remain sharp. Several tin pyrochlore solid solutions have also been studied (namely $Y_{2-y}Ln_ySn_2O_7$ where Ln = Sm, Nd, Pr, and Eu and $La_{2-y}Nd_ySn_2O_7$) by ^{119}Sn MAS NMR. When the short relaxation times of nuclei close to paramagnetic centers were exploited, a series of peaks were observed, associated with the substitution of paramagnetic for diamagnetic lanthanide ions in the local coordination around a tin atom. For $Y_{2-y}Sm_ySn_2O_7$ the composition of the solid solution could be determined from the intensities of these peaks. In the solid solutions the ^{119}Sn nuclei were found to be sensitive not only to neighboring paramagnetic ions but also to paramagnetic ions in the second and third coordination spheres. The shifts induced in these cases arise primarily from a through-space dipolar "pseudocontact" mechanism and can be interpreted with a model for the site symmetry based on the crystal structure.

Despite extensive exploitation of the paramagnetic properties of metal complexes[1,2] in NMR studies of molecules in solution, very few NMR experiments on such compounds in the solid state have been carried out. One reason for this is that it is often difficult to observe well-resolved NMR signals from paramagnetic solids, either because relaxation induced by the magnetic moments of unpaired electrons results in substantial line broadening or because large anisotropic interactions present in a solid (usually averaged by rapid molecular motion in solution) cause a large dispersion of the chemical shift in a powder sample. The lanthanides, however, form an important class of paramagnetic ions in this context because, with the exception of gadolinium, their electron relaxation (T_{1e}) times are sufficiently short for the nucleus to be coupled only weakly to the electronic spin system and relatively sharp resonances can be observed. Recently, ^{13}C NMR spectra of lanthanide acetates[3,4] have demonstrated that high-

[†] Chemical Crystallography Laboratory.
[‡] Inorganic Chemistry Laboratory.

(1) Hinckley, C. C. *J. Am. Chem. Soc.* **1969**, *91*, 5160-5162.
(2) Dobson, C. M.; Levine, B. A. *New Techniques in Biophysics and Cell Biology*; Pain, R. H., Smith, B. J., Eds.; Wiley-Interscience: New York, 1976; Vol. 3, pp 19-90.
(3) Chacko, V. P.; Ganapathy, S.; Bryant, R. G. *J. Am. Chem. Soc.* **1983**, *105*, 5491-5492. Ganapathy, S.; Chacko, V. P.; Bryant, R. G.; Etter, M. C. *J. Am. Chem. Soc.* **1986**, *108*, 3159-3165.
(4) Campell, G. C.; Crosby, R. C.; Haw, J. F. *J. Magn. Reson.* **1986**, *69*, 191-195.

0002-7863/89/1511-0505$01.50/0

Table I. Atomic Coordinates for the Pyrochlore Structure (with the Origin at the B Site)[11]

atom	location	site symmetry	coordinates		
			x	y	z
A	16d	D_{3d}	$^1/_2$	$^1/_2$	$^1/_2$
B	16c	D_{3d}	0	0	0
O	48f	C_{2v}	x	$^1/_8$	$^1/_8$
O′	8b	T_d	$^3/_8$	$^3/_8$	$^3/_8$

resolution spectra can be obtained and interpreted from these molecular structures in the solid state. In addition, we have reported ^{119}Sn MAS NMR spectra of the solid solution $Y_{2-y}Sm_ySn_2O_7$,[5] in which the chemical shifts of the ^{119}Sn nuclei were found to be extremely sensitive to the adjacent paramagnetic samarium ions, each successive substitution of Sm^{3+} for Y^{3+} into the local coordination sphere around the tin producing an additive shift.

Two dominant paramagnetic contributions to the lanthanide shift and relaxation effects in NMR spectra are expected, the relative importance of which will depend on the nature of the bonding in the compound. One contribution is the Fermi contact interaction between unpaired electrons of the paramagnetic ion and a given nucleus, which results from the delocalization of electron spin density on to the nucleus[6,7] and will therefore fall off very quickly as the number of bonds separating the resonating nucleus from the paramagnetic ion increases. This has been found to be the major contribution to shifts observed in the complete series of rare-earth phosphates and vanadates, which have been studied with ^{31}P and ^{51}V wide-line NMR.[8,9] The other contribution arises from the through-space dipolar interaction between the magnetic moments of unpaired electrons and the resonating nucleus. A "pseudocontact" shift can then result when a paramagnetic ion has an anisotropic magnetic susceptibility, which occurs when the symmetry of the ligand field at the lanthanide is less than cubic.[10]

In this paper we report a substantial extension to our study of $Y_{2-y}Sm_ySn_2O_7$ and examine in detail a wider series of lanthanide stannates. The compounds studied in this paper are all pyrochlores, of general formula $Ln_2Sn_2O_7$. The space group of the ideal pyrochlore is $Fd3m$, and all the atoms are on special positions whose coordinates are shown in Table I. The structure has only one positional parameter, the x parameter, which determines the location of one of the independent oxygen atoms (the 48f O atom). As the x parameter varies, the coordination around the cations alters. At one limit, when $x = 0.3125$ ($^5/_{16}$), the B site is perfectly octahedral, while at the other limit, when $x = 0.375$ ($^3/_8$), the coordination around A becomes a regular cube. The pyrochlore stannates, $Ln_2Sn_2O_7$, are known for all the lanthanides (except cerium) and also for yttrium.[12,13] In these pyrochlores, the Sn^{4+} cation is located on the 6-coordinated B site and the larger Ln^{3+} cation is on the 8-coordinated A site. It is possible to form solid solutions $Ln_{2-y}Ln'_ySn_2O_7$ with two (or more) lanthanide atoms on the A site. Only for lanthanides with similar ionic radii can complete solid solutions be formed.

In the present work, NMR studies have been carried out on the paramagnetic tin pyrochlores $Ln_2Sn_2O_7$, the solid solutions $La_{2-y}Nd_ySn_2O_7$ and $Y_{2-y}Eu_ySn_2O_7$, and the limited solid solutions $Y_{2-y}Sm_ySn_2O_7$, $Y_{2-y}Nd_ySn_2O_7$, and $Y_{2-y}Pr_ySn_2O_7$. There are three naturally occurring isotopes of tin, ^{115}Sn, ^{117}Sn, and ^{119}Sn, that have a spin of $I = ^1/_2$. The greater abundance (8.6%) and slightly greater sensitivity of ^{119}Sn makes this the more favorable NMR nucleus, and it has therefore been used in this study.

Table II. ^{119}Sn Isotropic Chemical Shifts for the Lanthanide Stannates, Together with Predicted Relative Magnitudes of the Contact and Pseudocontact Terms for the Different Lanthanides and Their Observed Magnetic Moments

ion		isotropic chemical shift, ppm	relative contact shift[a]	relative pseudocontact shift[b]	obsd magnetic moments at 300 K,[17] μ_B
$4f^0$	La^{3+}	−642	0.0	0.0	0.0
$4f^1$	Ce^{3+}	[c]	0.98	−6.3	2.3
$4f^2$	Pr^{3+}	−4150 ± 50	3.0	−11	3.4
$4f^3$	Nd^{3+}	−4160 ± 50	4.5	−4.2	3.5
$4f^4$	Pm^{3+}	[d]	4.0	2.0	
$4f^5$	Sm^{3+}	−92	−0.063	−0.7	1.6
$4f^6$	Eu^{3+}	4900 ± 200	−11	4.0	3.4
$4f^7$	Gd^{3+}	[e]	−32	0.0	7.9
$4f^8$	Tb^{3+}	[e]	−32	−86	9.5
$4f^9$	Dy^{3+}	[e]	−29	−100	10
$4f^{10}$	Ho^{3+}	[e]	−23	−39	10
$4f^{11}$	Er^{3+}	[e]	−15	33	9.4
$4f^{12}$	Tm^{3+}	1200 ± 400	−8.2	53	7.1
$4f^{13}$	Yb^{3+}	−690 ± 50	−2.6	22	4.9
$4f^{14}$	Lu^{3+}	−641	0.0	0.0	0.0
	Y^{3+}	−582	0.0	0.0	0.0

[a] The change in the effective magnetic field ΔH_c at the NMR nucleus, due to the Fermi contact interaction between a nucleus coordinated to a single lanthanide ion, can, to a first approximation, be assumed isotropic and is given by[16] (eq i) $\Delta H_c = (a_n\langle S_z\rangle)/(g_n\beta_n)$ where g_n is the nuclear gyromagnetic ratio, β_n the nuclear magneton, a_n the electron-nucleus hyperfine coupling constant, and $\langle S_z\rangle$ the average z component of the rare-earth spin. The numbers listed are the relative values for $\langle S_z\rangle$ calculated by Golding and Halton[16] and assume a_n to be constant across the lanthanide series. [b] The net pseudocontact shift for a lanthanide ion is given by[10] (eq ii) $\Delta H_p = (-g^2\beta^2J(J+1)(2J-1)(2J+3)FH_0)/(60(kT)^2r^{-3})$. g is the Landê g factor and F is an angular factor, which, for a system with axial symmetry, is equal to $A_2^0\langle r^2\rangle(3\cos^2\theta - 1)\langle J\|\propto\|J\rangle$, where θ is the angle between the principal magnetic axis of symmetry and the lanthanide–N internuclear axis, r the lanthanide–N distance (N is the resonating nucleus), $A_2^0\langle r^2\rangle$ is a crystal field parameter which can take a negative or positive value depending on the site symmetry, and $\langle J\|\propto\|J\rangle$ is a numerical coefficient. Here, the values quoted are those for $J(J+1)(2J-1)(2J+3)\cdot\langle J\|\propto\|J\rangle$; extra terms have been included to account for the mixing in of excited states (which is most important for the f^5 and f^6 ions, Sm^{3+} and Eu^{3+}) and the significant thermal population of the first excited state of Eu^{3+}. [c] No cesium(III) stannates exist. [d] $Pm_2Sn_2O_7$ was not synthesized. [e] No ^{119}Sn resonance could be detected.

Experimental Section

Polycrystalline samples of the pyrochlores were prepared from stoichiometric quantities of the rare-earth oxides and tin(IV) oxide. These were ground together and fired at 1350 °C for 4–5 days. The solid solutions required longer firing times (frequently of up to 2 weeks) and regrinding at least two or three times. The samples were then characterized by X-ray powder diffraction. Electron microscopy was carried out on a JEOL 2000FX analytical microscope with an energy dispersive X-ray detector.

The NMR spectra were collected on a Bruker CXP200 spectrometer operating at 74.5 MHz for ^{119}Sn. Magic angle spinning was carried out with approximately 0.7 g of sample, packed into Delrin Andrew-type rotors, using spinning speeds of approximately 4000 Hz.

Long recycle times, typically 30 s, were used to obtain spectra from the diamagnetic pyrochlores and good signal-to-noise ratios could be obtained in 200 scans. Spectra from the paramagnetic pyrochlores were accumulated by using much shorter recycle times (0.5–0.1 s) and large spectral widths (up to 200 kHz). Up to 15 000 scans were needed to obtain adequate signal-to-noise ratios in certain spectra, particularly in spectra from the $La_{1.8}Nd_{0.2}Sn_2O_7$ and $Y_{1.8}Eu_{0.2}Sn_2O_7$ samples.

Spin–lattice relaxation times were obtained by the inversion–recovery method.[14] Chemical shifts are quoted downfield from Me_4Sn and were measured for convenience from the MAS signal of polycrystalline SnO_2,

(5) Cheetham, A. K.; Dobson, C. M.; Grey, C. P.; Jakeman, R. J. B. *Nature (London)* **1987**, *328*, 706–707.
(6) McConnell, H. M.; Robertson, R. E. *J. Chem. Phys.* **1958**, *29*, 1361–1365.
(7) Kurland, R. J.; McGarvey, B. R. *J. Magn. Reson.* **1970**, *2*, 286–301.
(8) Bose, M.; Bhattacharya, M.; Ganguli, S. *Phys. Rev. B: Condens. Matter* **1979**, *19*, 72–79.
(9) Bose, M.; Ganguli, S.; Bhattacharya, M. *Phys. Rev. B: Condens. Matter* **1979**, *19*, 5335–5548.
(10) Bleaney, B. *J. Magn. Reson.* **1972**, *8*, 91–100.
(11) Subramanian, M. A.; Aravamudan, G.; Subba Rao, G. V. *Prog. Solid State Chem.* **1983**, *15*, 55–143.
(12) Whinfrey, C. G.; Eckart, D. W.; Tauber, A. *J. Am. Chem. Soc.* **1960**, *82*, 2695–2697.
(13) Whinfrey, C. G.; Tauber, A. *J. Am. Chem. Soc.* **1961**, *83*, 755–756.
(14) Vold, R. L.; Waugh, J. S.; Klein, M. P.; Phelps, D. E. *J. Chem. Phys.* **1968**, *48*, 3831–3832.

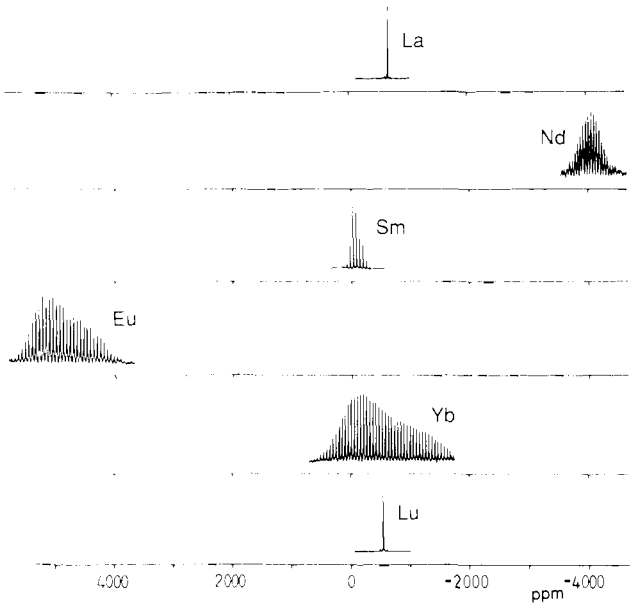

Figure 1. ^{119}Sn MAS NMR spectra of the pyrochlores $Ln_2Sn_2O_7$ at spinning speeds of 3-4 kHz, where Ln = La, Nd, Sm, Eu, Yb, and Lu. The chemical shifts are given relative to Me_4Sn.

which resonates at −604.3 ppm relative to Me_4Sn.[15]

Results and Discussions

1. Lanthanide Stannates $Ln_2Sn_2O_7$. The ^{119}Sn spectra from the pyrochlores $Ln_2Sn_2O_7$ (Ln = La, Nd, Sm, Eu, Yb, and Lu) are presented in Figure 1. When the optimum spectrometer parameters for accumulating spectra from diamagnetic tin(IV) pyrochlores were employed, the only paramagnetic sample that gave a detectable signal was $Sm_2Sn_2O_7$. However, when the recycle time was substantially reduced, the spectral width increased, and the spectral frequencies scanned systematically, spectra from a further five paramagnetic pyrochlores were found. Only one resonance is observed for each pyrochlore, consistent with there being only one crystallographically distinct tin site. $Pr_2Sn_2O_7$ and $Nd_2Sn_2O_7$ resonate ~3500 ppm upfield from the diamagnetic pyrochlores while all the others except $Yb_2Sn_2O_7$, which remains essentially unshifted, resonate downfield (Table II). The large number of sidebands observed in several of the spectra made it difficult to identify unambiguously the isotropic resonance for all the compounds, even by recording spectra at a variety of spinning speeds. The error limits quoted in Table II take into account this problem. The chemical shift range is much greater than that found for ^{119}Sn tin(IV) diamagnetic compounds[15] and is also 1 order of magnitude larger than the range observed in wide-line studies of rare-earth phosphates and vanadates.[8,9] The spin–lattice relaxation times are all considerably shorter than those of ~30 s found for the diamagnetic pyrochlores, that for $Sm_2Sn_2O_7$ being only ~0.002 s. However, an important feature of these spectra is the very narrow line widths of the individual peaks within the spinning sideband manifolds.

The isotropic shift of a paramagnetic compound will contain contributions from three major terms, namely the normal diamagnetic term, the Fermi contact term, and the pseudocontact (dipolar) term. The diamagnetic term is likely to alter across the lanthanide series as the size of the Ln^{3+} ion decreases. For the lanthanide stannates, however, the difference in ^{119}Sn chemical shifts between the extreme members of the lanthanide series (La and Lu), both diamagnetic pyrochlores, is only 79.5 ppm. The change in the diamagnetic term can therefore be assumed to be negligible in comparison to the shifts resulting from paramagnetic effects.

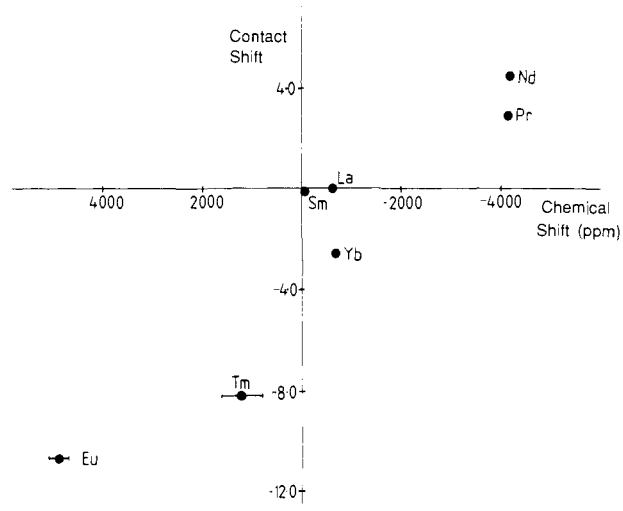

Figure 2. Plot of the theoretically predicted magnitude of the contact shift[16] versus the experimental isotropic chemical shift for the lanthanide stannates. The uncertainty in the isotropic chemical shift value is indicated by an error bar.

The experimentally observed values for the isotropic chemical shifts reverse sign between Nd^{3+} and Sm^{3+}, and there is little correlation between the experimental chemical shifts and the theoretically predicted relative magnitudes of the pseudocontact shift (Table II). Figure 2 shows, however, a plot of chemical shift of the tin pyrochlores against the theoretical (relative) values of the contact shift. The correlation is good. Thus, despite the tin atoms not being directly bonded to the lanthanide atoms, the contact term seems to be the dominant contribution to the paramagnetic shift. A similar correlation was found to exist in the study of ^{31}P shifts in rare-earth phosphates,[8] and deviations from perfect agreement with the theoretical values were ascribed to residual interactions, particularly to pseudocontact (dipolar) and local-field terms. Also, the relative values of the contact shift in Table II assume a constant value for the electron-nucleus hyperfine coupling constant, a_n; this is unlikely to hold in the pyrochlores because of both a decrease in cell length and an irregular increase in the x parameter across the lanthanide series. Finally, it should be noted that the pyrochlores whose signals proved impossible to locate were those with the largest predicted contact shifts.

The dramatic increase in the overall width of the ^{119}Sn resonances of the paramagnetic compounds compared to those from diamagnetic systems may similarly be explained on the basis of theoretical considerations. In these polycrystalline materials, the size of the interaction between the unpaired electron density and the resonating nucleus depends on the orientation of the individual crystallites with respect to the applied field. In solution, the thermal motion of the molecule averages these interactions. Magic angle spinning at accessible speeds does not however average these interactions completely but splits the broadened resonance into the spinning sideband manifold. The Fermi contact interaction is to a first approximation scalar, but the dipole field has an angular dependence and for a nucleus at distance r from a paramagnetic ion is given by[18]

$$H^d = \alpha(3\cos^2\theta - 1) \qquad (1)$$

where $\alpha = \mu^2 H_o/3kTr^3$ and θ the angle between the magnetic field and the axis linking the paramagnetic ion and the nucleus. (μ is the magnetic moment of the ion.) The susceptibility is here taken to be isotropic, which is a good approximation for the lanthanides, although the small anisotropy of the susceptibility is the origin of the pseudocontact contribution to the isotropic shift.[10] The overall widths of the resonance correlate well with the square of the magnetic moments of the lanthanides (see Table

(15) Fern, A. Part II Thesis, University of Oxford, 1986.
(16) Golding, R. M.; Halton, M. P. *Aust. J. Chem.* **1972**, *25*, 2577–2581.
(17) Figgis, B. N. *Introduction to Ligand Fields*; Wiley-Interscience: New York, 1966.
(18) Sobel, A. *J. Phys. Chem. Solids* **1967**, *28*, 185–196.

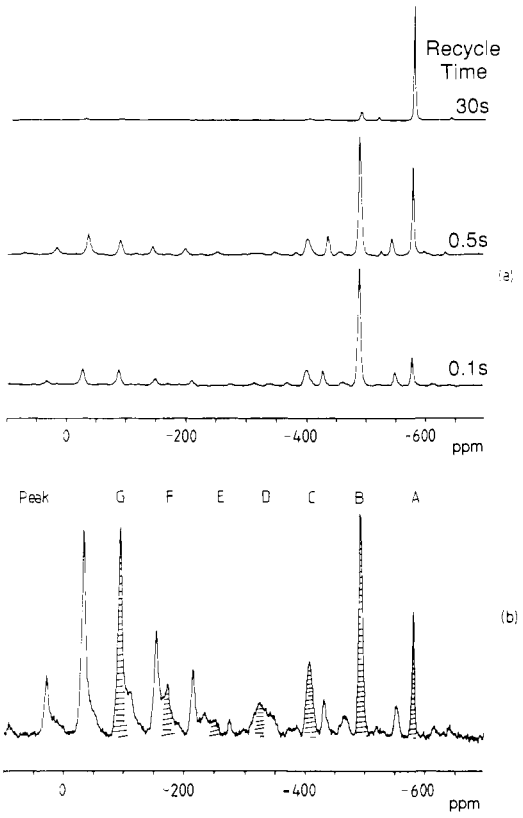

Figure 3. ^{119}Sn MAS NMR spectra from the preparation with stoichiometry $Y_{1.8}Sm_{0.2}Sn_2O_7$ obtained with recycle times of 30, 0.5, and 0.1 s. (b) ^{119}Sn MAS NMR spectrum of "$YSmSn_2O_7$" obtained with a recycle time of 0.5 s. The isotropic resonances A–G are shaded; the remaining peaks are spinning sidebands.

II). For example, $Sm_2Sn_2O_7$, which has only a small magnetic moment, shows a narrow resonance while $Yb_2Sn_2O_7$, which has a large magnetic moment, gives a very broad signal although the net shift of the latter from the diamagnetic position is smaller than that of the former. The dipolar mechanism does not, however, explain the broad line of $Eu_2Sn_2O_7$. Eu^{3+} has the largest contact shift of the lanthanides that we have studied, and the line width can be attributed to the small anisotropy of the contact interaction.

As well as giving large overall widths, both the dipolar interaction and the geometric part of the contact term can give rise to asymmetric line shapes;[18] such asymmetry is clearly observed in the spectra of $Sm_2Sn_2O_7$, $Eu_2Sn_2O_7$, and $Yb_2Sn_2O_7$ (Figure 1). It has however been demonstrated for static spectra that this asymmetry is only visible when the anisotropic interaction is larger than the "intrinsic line width" resulting from other causes of broadening. The latter may stem from local-field inhomogeneities[19-22] and also from the presence of other magnetic nuclei in the sample;[18] this may be the explanation for the lack of visible asymmetry in the spinning sideband manifold of $Nd_2Sn_2O_7$ (Figure 1) (and $Pr_2Sn_2O_7$, not shown, which has a similar line shape).

2. Pyrochlore Solid Solutions. The systems $Y_{2-y}Sm_ySn_2O_7$, $Y_{2-y}Nd_ySn_2O_7$, $Y_{2-y}Pr_ySn_2O_7$, $Y_{2-y}Eu_ySn_2O_7$, and $La_{2-y}Nd_ySn_2O_7$ have been studied in detail. Powder X-ray diffraction of these samples shows that Sm^{3+}, Nd^{3+}, and Pr^{3+} form only very limited solid solutions in $Y_2Sn_2O_7$, while Nd^{3+} and Eu^{3+} form complete solid solutions in $La_2Sn_2O_7$ and $Y_2Sn_2O_7$, respectively. X-ray microanalysis confirmed the lack of any new phases and the homogeneity of each sample.

Since $Sm_2Sn_2O_7$ resonates at −92 ppm, only ~500 ppm downfield from the diamagnetic pyrochlores, and has the smallest

(19) Stoll, M. E.; Majors, T. J. *Phys. Rev. B: Condens. Matter* **1981**, *24*, 2859–2862.
(20) Drain, L. E. *Proc. Phys. Soc., London* **1962**, *80*, 1380–1382.
(21) Kroon, D. J. *Philips Res. Rep.* **1960**, *15*, 501–583.
(22) Alla, M.; Lippmaa, E. *Chem. Phys. Lett.* **1982**, *87*, 30–33.

Table III. Spin–Lattice Relaxation (T_1) Times of the More Intense Peaks in the Spectrum of the Sample with Stoichiometry $YSmSn_2O_7$

resonance	spin–lattice relaxation time (T_1), s	resonance	spin–lattice relaxation time (T_1), s
peak A	16	peak C	0.006
peak B	0.011	peak G	0.0006

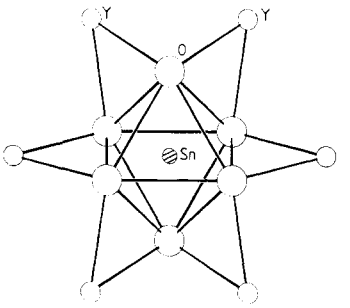

Figure 4. Local environment of the tin atom in $Y_2Sn_2O_7$, showing the six nearest yttrium atoms coordinated to the SnO_6 octahedron.

sideband intensity of all the paramagnetic stannates, the $Y_{2-y}Sm_ySn_2O_7$ system was the first to be studied. The two end members resonate within 500 ppm of each other, and it was possible to observe the whole range of frequencies in this system in spectra recorded with a 75-kHz sweep width. Figure 3a shows ^{119}Sn spectra of one preparation from the phase diagram $Y_{2-y}Sm_ySn_2O_7$ with stoichiometry $Y_{1.8}Sm_{0.2}Sn_2O_7$ and illustrates the effect of varying the recycle time on the spectra accummulated. As the recycle time is reduced, signals from nuclei with long relaxation times are saturated and the relative intensities of signals from nuclei with fast relaxation times increase. In a sample of mean composition $YSmSn_2O_7$, seven resonances become visible (Figure 3b) when the recycle time is sufficiently fast (0.5 s). The spin–lattice relaxation times (T_1 values) of the more intense peaks in this $YSmSn_2O_7$ sample were measured, and the results are recorded in Table III. The T_1 value for peak A is only slightly less than the T_1 values (of nearly 30 s) obtained for the diamagnetic pyrochlores. There is a sudden decrease in relaxation time between peak A and peak B, followed by a more steady decrease from peaks B to C to G.

In order to rationalize the spectra obtained from the pyrochlore solid solutions, the coordination around the tin atoms in the pyrochlore structure has to be considered. Figure 4 shows that the central tin atom is coordinated through oxygen atoms to six equivalent lanthanide atoms. The $Y_{2-y}Sm_ySn_2O_7$ ^{119}Sn spectra can now be explained as follows. The resonance at −582 ppm, peak A in Figure 3, is at the same position as the single resonance observed for $Y_2Sn_2O_7$, and peak G in the spectra is in the same position as the resonance observed for $Sm_2Sn_2O_7$. The new peaks B–F result from changes in the local coordination when Sm^{3+} substitutes for Y^{3+} in $Y_2Sn_2O_7$ and can be assigned to tin atoms with the following local environments: $Sn(OY)_5(OSm)$ [peak B], $Sn(OY)_4(OSm)_2$ [peak C], $Sn(OY)_3(OSm)_3$, [peak D], $Sn(OY)_2(OSm)_4$ [peak E], $Sn(OY)(OSm)_5$ [peak F].[5] The progressive substitution of samarium atoms into the local environment around the tin atoms also provides an explanation for the decrease in T_1 values from peak A to peak G. The intensities of the seven resonances obtained from spectra collected under conditions of full relaxation of all the atoms between each pulse can be directly related to the number of tin atoms with particular local environments. The intensities of peaks A–C (peak D was not detectable above the noise in this experiment) were used to determine the limit of solid solution of $Sm_2Sn_2O_7$ in $Y_2Sn_2O_7$, which had proved impossible from powder X-ray diffraction data; this gave an estimate of $Y_{1.85}Sm_{0.15}Sn_2O_7$. The intensities of peaks G, F, and E were used to obtain a value of only $Y_{0.03}Sm_{1.97}Sn_2O_7$, for $Y_2Sn_2O_7$ in $Sm_2Sn_2O_7$.

Spectra of samples from the phase diagrams $Y_{2-y}Nd_ySn_2O_7$, $La_{2-y}Nd_ySn_2O_7$, $Y_{2-y}Pr_ySn_2O_7$, and $Y_{2-y}Eu_ySn_2O_7$ were also re-

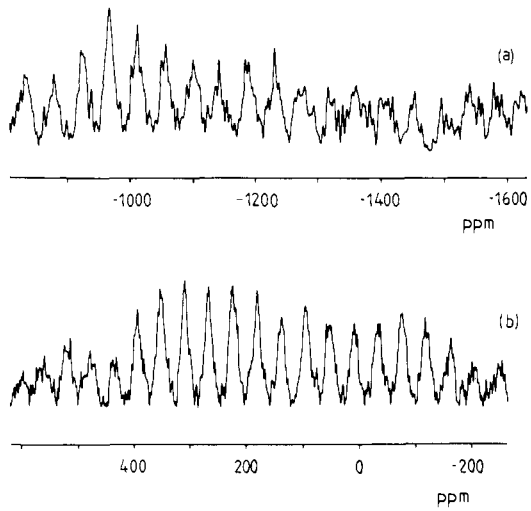

Figure 5. ^{119}Sn MAS NMR spectra of $La_{1.8}Nd_{0.2}Sn_2O_7$ (a) and $Y_{1.8}Eu_{0.2}Sn_2O_7$ (b) collected with short recycle times of 0.1 s and spectral offsets centered around −1100 and −200 ppm, respectively.

corded. The complete spectra will not be presented separately, but spectra that exemplify three different observations will be grouped together.

Figure 5 shows resonances from the samples $La_{1.8}Nd_{0.2}Sn_2O_7$ and $Y_{1.8}Eu_{0.2}Sn_2O_7$ at approximately −1150 and 250 ppm, respectively. The resonance in the spectrum of the $La_{1.8}Nd_{0.2}Sn_2O_7$ sample (Figure 5a) has shifted approximately 500 ppm from the $La_2Sn_2O_7$ resonance, approximately $^1/_6$ of the shift between the $La_2Sn_2O_7$ and $Nd_2Sn_2O_7$ (at 4164 ppm) resonances. Similarly, in the $Y_{1.8}Eu_{0.2}Sn_2O_7$ spectrum, the resonance at ~250 ppm also represents a shift downfield of approximately $^1/_6$ of the shift between $Y_2Sn_2O_7$ and $Eu_2Sn_2O_7$, at 4900 ppm. The ^{119}Sn spectrum from $Y_{1.8}Nd_{0.2}Sn_2O_7$ contained a resonance at approximately the same chemical shift as the analogous lanthanum system, but the signal to noise was poor, because of the limited incorporation of Nd^{3+} into $Y_2Sn_2O_7$. The resonances observed are therefore attributed to substitution of one paramagnetic ion into the local environment around the tin atoms and are analogous to peak B in the $Y_{2-y}Sm_ySn_2O_7$ ^{119}Sn spectra. Because of the poor signal-to-noise ratio and the very broad resonances obtained, the search for resonances analogous to peak C in the $Y_{2-x}Sm_xSn_2O_7$ spectra was not pursued.

The ^{119}Sn spectra for the samples with stoichiometry $Y_{1.8}Nd_{0.2}Sn_2O_7$ and $Y_{1.5}Nd_{0.5}Sn_2O_7$, collected with a long recycle time of 30 s, are displayed in Figure 6a, together with the spectrum of $Y_2Sn_2O_7$ for a comparison. All three spectra contain a resonance at −582 ppm attributed to $Sn(OY)_6$: the incorporation of Nd^{3+} ions into $Y_2Sn_2O_7$ does not cause a shift in this peak. There is, however, an increasing intensity of the spinning sidebands with increasing amount of Nd^{3+} present in the samples, but the individual peaks are sharp and the spin–lattice relaxation times (T_1) of the resonances remain essentially unchanged for the three samples. Figure 6b shows the spectrum, collected under the same conditions as those used in Figure 6a, of a mixture of 25% $Nd_2Sn_2O_7$ and 75% $Y_2Sn_2O_7$, which were prepared separately and then ground together. There is again a marked increase in the intensity of the sidebands of the resonance from the $Y_2Sn_2O_7$ phase (at −582 ppm), despite there being no paramagnetic ions directly incorporated into $Y_2Sn_2O_7$ crystallites. The T_1 value of the resonance is unaffected, within the limits of the measurements, by mixing with $Nd_2Sn_2O_7$. The similar behavior of these two samples suggests that the increase in the overall line width in the $Y_{2-y}Nd_ySn_2O_7$ samples arises from distant Nd^{3+} ions not necessarily in the $Y_2Sn_2O_7$ lattice but also from the $Nd_2Sn_2O_7$ present in the sample. This susceptibility broadening has been observed in the ^{29}Si and ^{27}Al spectra of zeolites[23] and also in the ^{13}C spectra

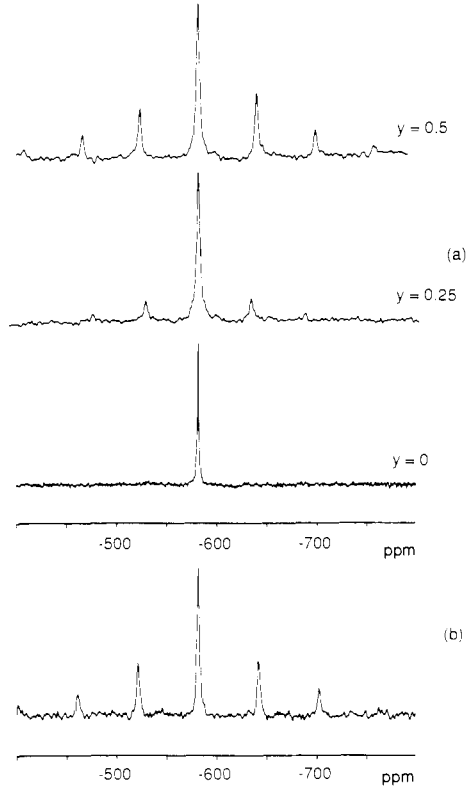

Figure 6. ^{119}Sn MAS NMR spectra of (a) $Y_{2-y}Nd_ySn_2O_7$ with stoichiometry y = 0 ($Y_2Sn_2O_7$), 0.2, and 0.5 and (b) an unfired mixture of 75% $Y_2Sn_2O_7$ and 25% $Nd_2Sn_2O_7$. All spectra were accumulated with a 30-s recycle time between pulses and a spectral offset centered close to −582 ppm.

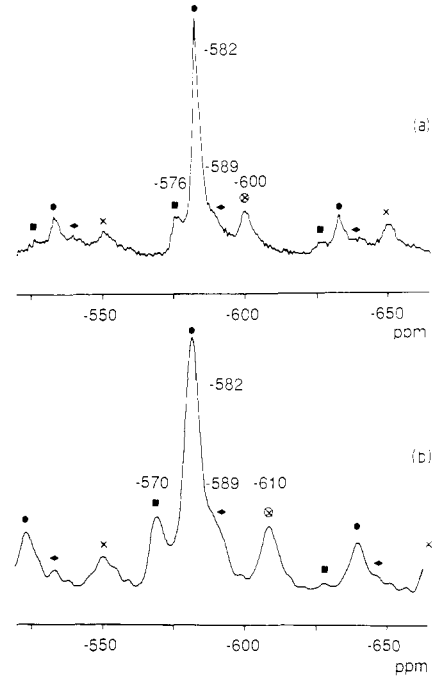

Figure 7. ^{119}Sn MAS NMR spectra of the $Y_{1.8}Nd_{0.2}Sn_2O_7$ (a) and $Y_{1.5}Pr_{0.5}Sn_2O_7$ (b) samples collected with a short recycle time of 0.1 s. The values of the chemical shifts of the isotropic resonances are marked; the remaining peaks are spinning sidebands.

of adamantane,[24] in samples containing paramagnetic ions.

A careful inspection of the $Sn(OY)_6$ resonance in the spectrum from the $Y_{1.8}Nd_{0.2}Sn_2O_7$ sample, observed by using a very short recycle time of 0.1 s, shows that though the resonance at −582

(23) Oldfield, E.; Kinsey, R. A.; Smith, K. A.; Nichols, J. A.; Kirkpatrick, R. J. *J. Magn. Reson.* **1983**, *51*, 325.

(24) Ganapathy, S.; Bryant, R. G. *J. Magn. Reson.* **1986**, *70*, 149–152.

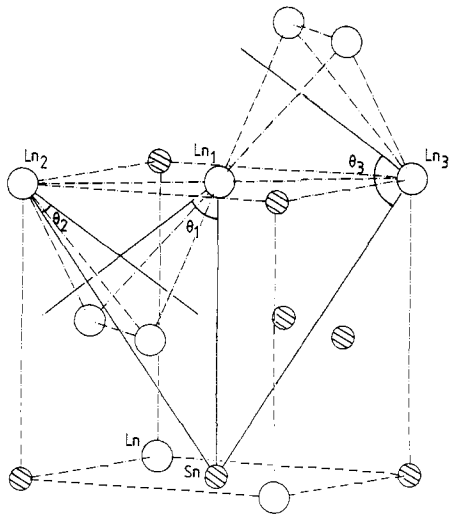

Figure 8. $^1/_8$ of the unit cell of a lanthanide tin(IV) pyrochlore showing four of the nearest lanthanide atoms and three of the 18 next-nearest lanthanide atoms (Ln_1, Ln_2, and Ln_3). The angles θ_1, θ_2, and θ_3 between the Ln–Sn internuclear axis and the C_3 symmetry axis at the Ln atom are shown.

ppm still dominates the spectrum, there are additional resonances, one downfield of the main resonance at −582 ppm with an isotropic chemical shift of −576 ppm and one upfield at −600 ppm (Figure 7a). Resolution enhancement of the free induction decay shows, more clearly, a further peak at −589 ppm, just visible in Figure 7a. These new resonances have shorter T_1 values than the peak at −582 ppm, since they are only observable in spectra collected with very short recycle times. Three additional resonances can also be seen in the spectrum of the $Y_{1.8}Pr_{0.2}Sn_2O_7$ sample shown in Figure 7b. There is again a peak just discernable at −589 ppm and a further two resonances at −570 and −610 ppm. The two outer peaks (at −570 and +610 ppm) have shifted further from the $Y_2Sn_2O_7$ resonance than have the corresponding resonances in the spectra of the $Y_{2-y}Nd_ySn_2O_7$ samples shown in Figure 7a.

Since Nd^{3+} ions not physically incorporated into a particular crystallite have been found not to affect the relaxation times of the tin nuclei in this system, these additional resonances must result from tin in crystallites containing paramagnetic ions. These paramagnetic ions cannot be substituted into the first lanthanide coordination sphere around the tin atom, as this would cause the massive shifts observed earlier. They could, however, be substituted into the next coordination sphere.

Though shifts resulting from paramagnetic ions in the first coordination sphere have been found to be primarily due to contact interactions, the pseudocontact contribution to the shift is likely to become increasingly important relative to the contact contribution, as the number of bonds separating the paramagnetic ion and the resonating nucleus increases. The pseudocontact term has a r^{-3} dependence on distance but also depends upon the angles between the principal magnetic axes at the lanthanide and the lanthanide–tin vector (see eq ii, Table II); it can therefore take both negative and positive values for the same lanthanide ion, depending on the structure. This would account for the observation of both upfield and downfield shifts from the peak at −582 ppm in Figure 7.

There are six lanthanide atoms in the second coordination shell around a central tin atom, of which one, marked Ln_1, is shown in Figure 8; these are located at a distance $a_0/2$, where a_0 is the unit cell length, from Sn. The third coordination shell comprises 12 rare-earth ions at $a_0/2$ from Sn; these can be grouped into two sets of six, marked Ln_2 and Ln_3 in Figure 8, as described below. It is plausible to suggest that substitution of a paramagnetic ion in these sites might result in one of three different resonances.

Since the symmetry at the lanthanide site in the pyrochlore structure is D_{3d} ($\bar{3}m$), and therefore axial, the pseudocontact term has, on the assumption that the principal axis of the magnetic moment at the lanthanide ion lies along the symmetry axes at the lanthanide atom site, an angular factor proportional to $3\cos^2\theta - 1$ (see eq ii, Table II),[10] where θ is the angle between the Sn–Ln interatomic axis and the principal 3-fold axis at the lanthanide. The six atoms in the first coordination sphere are equivalent and have $\theta = 90°$. Any pseudocontact contribution to the shift arising from substituting progressively more paramagnetic lanthanide ions into the local environment around a tin atom will therefore simply be additive. The values for θ for the three magnetically different lanthanide sites in the second and third spheres are 54.74, 19.47, and 90° for Ln_1, Ln_2, and Ln_3, respectively. These three angles, marked θ_1, θ_2, and θ_3 in Figure 8, give values for $3\cos^2\theta - 1$ of 0.0, 1.667, and −1.0, respectively. A shift due to a substitution at Ln_1 does not therefore have a pseudocontact contribution while substitution at Ln_2 and Ln_3 will produce downfield and upfield pseudocontact contributions to the overall shifts.

We can then tentatively suggest that the two peaks at −576 and −600 ppm in the $Y_{1.8}Nd_{0.2}Sn_2O_7$ compound result from substitution of one Nd^{3+} ion into the Ln_2 or Ln_3 sites. The much larger shifts observed from the $Y_{1.8}Pr_{0.2}Sn_2O_7$ sample are in agreement with the predicted magnitudes of pseudocontact shifts calculated by Bleaney[10] (see Table II). There is also presumably a small contact term present in these shifts caused by substitution into the second coordination sphere. Hence, substitution in the Ln_1 site will produce a small upfield shift, which provides an explanation for resonance at −589 ppm in the $Y_{1.8}Nd_{0.2}Sn_2O_7$ and $Y_{1.8}Pr_{0.2}Sn_2O_7$ systems. As to whether substitution at Ln_2 produces a downfield or upfield shift will depend on the sign of the crystal field parameter, $A_2^0\langle r^2\rangle$. For pyrochlores, with space group $Fd3m$, this is positive,[25] and substitution at Ln_2 will therefore produce a downfield shift and Ln_3 an upfield shift.

Conclusions

Shifts in the ^{119}Sn MAS NMR spectra of lanthanide stannates have been observed resulting from the substitution of paramagnetic for diamagnetic ions in the primary coordination sphere around a tin atom. The shifts were found to be predominantly caused by a Fermi contact interaction, implying a small covalent interaction between the lanthanide ion and the ^{119}Sn atom. The magnitudes of shifts obtained are massive compared with those associated with substitution of diamagnetic cations in the primary sphere of this and other systems (for instance in the ^{29}Si NMR spectra of zeolites[26]). The dispersion of chemical shifts has clear analogies with solution paramagnetic shift probes,[1,2] and it is hoped that the use of paramagnetic ions to increase the resolution in solid-state NMR will be widely applicable. In the present example, intensities of the various resonances in the NMR spectra could be used to quantify accurately the distribution of rare earths within the structure, and the limits of the solid solutions could be estimated. This approach has obvious potential in systems where the distributions of rare-earth ions is of importance for understanding the properties of the materials involved, for example, in laser materials, phosphors, and host materials for fission product elements.[27-29]

Shifts were also observed, associated with the substitution of paramagnetic lanthanides into the second and third coordination spheres around a tin atom. These shifts contain substantial contributions from a dipolar (pseudocontact) mechanism and can be understood by detailed consideration of the pyrochlore structure. The magnitude and direction of such shifts can be used, in principle, to obtain detailed geometric information about the relative position of the NMR nucleus and the lanthanide ion.

As well as shifts of resonances, the paramagnetic ions were found to cause significant reduction in spin–lattice relaxation rates of the ^{119}Sn atoms. This enabled spectra to be collected in a much

(25) Chien, C. L.; Sleight, A. W. *Phys. Rev. B: Condens. Matter* **1978**, *18*, 2031.
(26) Lippmaa, E.; Magi, M.; Samosan, A.; Engelhardt, G.; Grimmer, A.-R. *J. Am. Chem. Soc.* **1980**, *102*, 4889–4893.
(27) Leone, S. R.; Moore, C. B. *Chemical and Biochemical Applications of Lasers*; Moore, C. B., Ed.; Academic: New York, 1974; pp 1–27.
(28) Blasse, G.; Bril, A. *Philips Tech. Rev.* **1970**, *10*, 304–332.
(29) Ringwood, A. E.; Kesson, S. E.; Ware, N. G.; Hibberson, W.; Major, A. *Nature (London)* **1979**, *278*, 219–223.

shorter time than for diamagnetic samples. This approach, similar to that used in glasses,[30] should be of value in other crystalline systems where long relaxation times limit the sensitivity of the NMR method. The resonances of different species close to the paramagnetic centers could be selectively observed by varying the recycle times between pulses and saturating selectively the resonances of nuclei far from the paramagnetic ions. When this approach is used, resonances could for example be detected from ^{119}Sn nuclei in local environments with very low concentrations in the solid. This ability to observe the fast relaxing nuclei despite their low abundance, should be of particular value in cases where paramagnetic ions are incorporated only in trace concentrations within a solid.

Overall, this study has demonstrated the potential of MAS NMR in the study of paramagnetic continuous solids and suggests that incorporation of paramagnetic centers can offer a novel approach to the characterization of 3D materials by MAS NMR.

Acknowledgment. We thank the SERC for the provision of a research studentship for C.P.G. and a grant toward the purchase of the NMR equipment, A. Stoker for help with the X-ray microanalysis, and S. J. Heyes and J. M. Twyman for valuable advice concerning the NMR experiments.

(30) Fujiu, T.; Ogino, M. *J. Non-Cryst. Solids* **1984**, *64*, 287-290.

Mechanism of the Claisen Rearrangement of Allyl Vinyl Ethers

Michael J. S. Dewar* and Caoxian Jie

Contribution from the Department of Chemistry, The University of Texas at Austin, Austin, Texas 78712. *Received February 15, 1988. Revised Manuscript Received August 12, 1988*

Abstract: AM1 calculations are reported for the Claisen rearrangements of allyl vinyl ether and 23 derivatives. The reactions are predicted, correctly, to take place preferentially via chair-type transition states and to lead preferentially to E isomers. While some of the reactions are predicted to take place by two alternative paths, corresponding to alternative synchronous and nonsynchronous mechanisms, involving transition states that are, respectively, aromatic and biradicaloid, the distinction here is only marginal, and most of the reactions took place by a single unique path of intermediate type.

The Claisen rearrangement (CLR) of allyl vinyl ethers to γ,δ-unsaturated carbonyl compounds (e.g. **1** → **2**; Chart I) bears an obvious formal analogy to the Cope rearrangement (COR) of 1,5-hexadienes (e.g. **3**). Both reactions are concerted,[1] taking place via transition states (TS) with chair-type geometries,[2,3] and it was formerly assumed that both are synchronous,[1] being typical "allowed"[4] pericyclic reactions with aromatic[5] TSs (**5** and **6**). However, experimental[6] and theoretical[7] studies in these laboratories showed some years ago that the COR normally takes place by an alternative nonsynchronous mechanism first suggested by Doering et al.[8] where the symmetrical intermediate is a biradicaloid derived from the biradical (**7**) by through-bond interactions between the radical centers. This was a surprising conclusion because it had been generally assumed that "allowed" pericyclic reactions are always synchronous unless the synchronous path is inaccessible for steric reasons.

A possible explanation of this apparent anomaly was given recently in the form of a new reaction rule,[9] that multibond reactions are not normally synchronous, a multibond reaction being one where two or more bonds are formed or broken. The rationale for this is that activation barriers for reactions are due to the need to weaken bonds that break during the reaction before new bonds can begin to form. The activation energy of a synchronous two-bond reaction should then be roughly double that of an analogous one-bond one.

Chart I

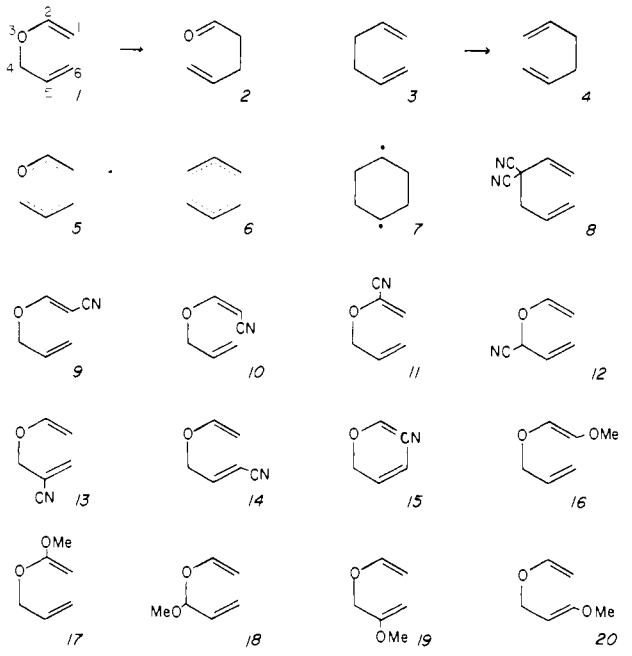

(1) A *concerted* reaction is one that takes place in a single kinetic step. A *synchronous* reaction is a concerted reaction in which all changes in bonding have taken place to comparable extents in the transition state. A *two-stage* reaction is one which is concerted but not synchronous; some changes in bonding taking place mainly before, and some mainly after, the transition state.

(2) Doering, W. v. E.; Roth, W. R. *Tetrahedron* **1962**, *18*, 67.

(3) Hansen, H.-J.; Schmid, H. *Tetrahedron* **1974**, *30*, 1959.

(4) Woodward, R. B.; Hoffmann, R. *Angew. Chem., Int. Ed. Engl.* **1969**, *8*, 781.

(5) (a) Evans, M. G.; Warhurst, E. *Trans. Faraday Soc.* **1938**, *34*, 614; (b) Dewar, M. J. S. *Angew. Chem., Int. Ed. Engl.* **1971**, *10*, 761.

(6) Dewar, M. J. S.; Wade, L. E., Jr. *J. Am. Chem. Soc.* **1977**, *99*, 4417.

(7) Dewar, M. J. S.; Ford, G. P.; McKee, M. L.; Rzepa, H. S.; Wade, L. E., Jr. *J. Am. Chem. Soc.* **1977**, *99*, 5069.

(8) Doering, W. v. E.; Toscano, V. G.; Beasley, G. H. *Tetrahedron* **1971**, *27*, 299.

(9) Dewar, M. J. S. *J. Am. Chem. Soc.* **1984**, *106*, 209.

0002-7863/89/1511-0511$01.50/0